Bachelorarbeit

Institut für Theoretische Physik
Computational Physics

Visualization of a simplified terrestrial planet formation model including gravitational force and collisions

Advisor:
Univ.-Prof. Enrico Arrigoni

Theresa Mayer

Mat.Nr. 11777178

Sommersemester 2022

Contents

Abstract

In this thesis a simplified visualization of the terrestrial planet formation from planetary embryos to planets is presented. The program is written in python and results are visualized using vpython. The purpose is to develop intuition for the role of gravity and collision in planet formation. To analyse the accuracy of the program the results are compared with the analytic solution of the two body problem and the conservation of integrals is tested.

1 Motivation

The goal of thesis is to give a visual insight into the terrestrial planet formation. To realise this a program calculating the time evolution and visualizing it was written. To analyse its accuracy the results are compared to the analytically solvable two-body problem and the conservation of integrals is tested.
It should be noted, that this simulation is not intended to depict real formations of planetary systems. There are to reasons for this. First, for a more realistic situation one has to consider effects which come with large computational efforts which would go beyond the scope of this thesis. Second, this simulation should serve as a tool to help build intuition for the problem.

2 Introduction

The aim of this thesis is to illustrate how a planetary system evolves from a system containing many planetary embryos to a system of few planets. A very simplified approach is chosen, which only considers the classical gravitational force between massive objects. All collisions are handled as total inelastic collisions. The implications of these simplifications will be discussed in section 3.5.

2.1 Terrestrial Planet Formation

The following information is taken from [5]. See also [7] for more information.
In the early stages the sun is surrounded by a protoplanetary disk consisting of gas as well as dust grains and ice particles. The first growth stage is dominated by hit and stick collisions between dust grains and ice particles, forming particles up to millimeter and centimeter sizes.

One idea to explain the growth up to meter and kilometer sizes, objects known as planetesimals is formation by gravitational collapse.
To reach the size of planetary embryos there are two different growth regimes. Either by planetesimal-planetesimal collision or by planetesimals accreting the remaining small dust pebbles. Pebble accretion can be much faster and may, therefore explain the formation of gas giant cores, since these have to form before the gaseous disk dissipates.
In the third stage planetary embryos evolve to planets. Typical masses for planetary embryos are between lunar and Mars-like masses. This growth stage is marked by violent giant collisions. This thesis focuses on the simulation of this large stage.

2.2 Theoretical description

In the following the necessary relations for computation are given, taken from [2], see also [9],[3].

2.2.1 N-body problem

In this thesis the case of a planetary system where N-1 objects revolve around one sun is realized. The system is described by N objects interacting with each other via a gravitational force. This is called the N-body problem.
According to Newton's laws

$$m_\nu \mathbf{a}_\nu = \mathbf{F}_\nu \tag{1}$$

$$\mathbf{F}_\nu = \sum_{\mu \neq \nu}^{N} \mathbf{F}_{\nu\mu} \tag{2}$$

$$\mathbf{F}_{\nu\mu} = -\frac{G m_\nu m_\mu}{r_{\nu\mu}^2} \hat{\mathbf{r}}_{\nu\mu} \tag{3}$$

Here $\mathbf{F}_\nu$ is the total force acting on m_ν, which is given by the sum over the individual forces between all objects $\mathbf{F}_{\nu\mu}$, in this case given by the gravitational force (3) and $\mathbf{r}_{\nu\mu}$ points from m_μ to m_ν.
This set of differential equations can not be solved analytically. Therefore, numerical methods have to be used.
The choice of initial conditions for $\mathbf{r}_\nu$ and $\dot{\mathbf{r}}_\nu$ are described in section 3.2.

2.2.2 Collisions

Collisions are considered to be inelastic. After a collision occurred instead of two objects with masses m_1 and m_2 a new more massive object with $M = m_1 + m_2$ exists. The new initial velocity is chosen in a way that conserves the total momentum.

$$m_1 \mathbf{v_1} + m_2 \mathbf{v_2} = M \mathbf{v} \tag{4}$$

Furthermore, the center of mass (9) gives the new position of the new object. The total energy and total angular momentum are not conserved during an inelastic collision.

2.2.3 Integrals

The planetary system considered is a closed system, i.e. no external forces, therefore total momentum and total angular momentum are conserved. Furthermore, gravitational forces are conservative and the total energy is conserved as well. Consequently, the integrals are given by:

$$\mathbf{P} = \sum_{i}^{N} m_i \dot{\mathbf{r}}_i = const. \tag{5}$$

$$\mathbf{L} = \sum_{i}^{N} m_i \mathbf{r} \times \dot{\mathbf{r}}_i = const. \tag{6}$$

$$E = T + U = \sum_{i}^{N} \frac{m_i \dot{r}_i^2}{2} - \frac{1}{2} \sum_{\nu,\mu \neq \nu}^{N} \frac{G m_\nu m_\mu}{r_{\nu\mu}} = const. \tag{7}$$

2.3 Methods

As mentioned above, there is no analytical solution for $N > 3$. For this reason, the time evolution is calculated numerically. The program is written in python, see section 3.1 for more details. For the graphical simulation of the evolution of the system the vpython (visual python) package was used.
As integration algorithm the Strömer-Verlet method was used. It is a two step algorithm given by

$$\begin{aligned} \dot{\mathbf{r}}_{n+1/2} &= \dot{\mathbf{r}}_{n-1/2} + \mathbf{a}(\mathbf{r}_n)\Delta t \\ \mathbf{r}_{n+1} &= \mathbf{r}_n + \dot{\mathbf{r}}_{n+1/2}\Delta t \end{aligned} \tag{8}$$

For more details see [4]. In section 3.1.1 the advantages and disadvantages of this algorithm are discussed in more detail.

2.3.1 Analytical solution

Kepler Problem

Here two objects interacting with each other via the gravitational force are considered. The following arguments and relations are taken from [2] See also [9][3]
In three dimension two bodies have $2 \cdot 3 = 6$ degrees of freedom. However, there are five conserved quantities: conservation of total momentum, total angular momentum and total energy. Respectively, reducing the problem to: one particle, radial equation (confined to one plain) and first order differential equation. The solution of the differential equation can be given in form of an integral.
An analytic expression relating the two cartesian coordinates of one object, giving their orbitals. This can be done using the following formulas.

In the following the motion of the objects is restricted to the xy-plane and $\mathbf{r_1}$ and $\mathbf{r_2}$ describe the position of object 1 and 2 in cartesian coordinates. The relative coordinate $\mathbf{r}$ and center of mass $\mathbf{R}$ are given by

$$\mathbf{R} = \frac{m_1\mathbf{r_1} + m_2\mathbf{r_2}}{m_1 + m_2}, \qquad \mathbf{r} = \mathbf{r_1} - \mathbf{r_2} \tag{9}$$

which can be related to $\mathbf{r_1}$ and $\mathbf{r_2}$ using

$$\mathbf{r_1} = \mathbf{R} + \frac{m_2}{m_1 + m_2}\mathbf{r}, \qquad \mathbf{r_2} = \mathbf{R} - \frac{m_1}{m_1 + m_2}\mathbf{r} \tag{10}$$

Using the Lagrange formalism, exploiting the conserved quantities and choosing cylindrical coordinates for the relative coordinates $\mathbf{r} = \rho cos(\phi)\mathbf{e_x} + \rho sin(\phi)\mathbf{e_y} + z\mathbf{e_z}$ leads to the following time dependent relations:

$$z(t) = 0 \tag{11}$$

$$\dot{\mathbf{R}} = const. \tag{12}$$

$$\dot{\phi} = \frac{l}{\mu\rho(t)^2} \tag{13}$$

$$\dot{\rho} = \sqrt{\frac{2}{\mu}\left(E - \frac{l^2}{2\mu\rho(t)^2}\right) - U(\rho)} \tag{14}$$

as well as a relation between ρ and ϕ describing the orbital motion in the xy-plain

$$\frac{p}{\rho} = 1 + \epsilon cos(\phi) \tag{15}$$

where

$$p = \frac{l^2}{\mu\alpha}, \quad \epsilon = \sqrt{1 + \frac{2El^2}{\mu\alpha^2}} \tag{16}$$

l ... total angular momentum
E ... total energy
μ ... reduced mass $\frac{m_1 m_2}{m_1+m_2}$
α ... Gm_1m_2

There are three different forms of the orbital motion described by (16).

$$\begin{aligned} \epsilon > 1 \quad E > 0 \quad Hyperbola \\ \epsilon = 1 \quad E = 0 \quad Parabola \\ \epsilon < 1 \quad E < 0 \quad Ellipse \end{aligned} \tag{17}$$

For elliptical orbits is is possible to find an expression for the period.

$$\tau = \frac{2\pi a^{\frac{3}{2}}}{\sqrt{G(m_1 + m_2)}}, \quad a = \frac{p}{1 - \epsilon^2} \tag{18}$$

3 Calculations and Results

3.1 The Program

In this section a brief description of the program is given. It is written in python. The program is a simple simulation of the evolution of an early planetary system containing one star and planetary embryos. It takes into account the gravitational force and collisions in the form of total inelastic collisions between all objects. The units are given in: $[t] = anno$, $[length] = AU$, $[mass] = m_{sun}$.
The program can be split into three parts: creating the initial system, integrating over time and simulating the results. To give an overview, the program will be explained in the order of the program flow.

Initial system First, an intital random system is created, with parameters which can be chosen according to section 3.2. The parameters are:

- minimal and maximal mass of initial planetary embryos
- mass of the star
- minimal and maximal minimal distance of planetary embryos from the star

- maximal eccentricity
- maximal inclination

Within these parameters the properties of the planetary embryos are chosen randomly via a uniform distribution. The initial velocity of the sun is set to zero. The initial velocities of the planetary embryos are calculated according to the two body problem between sun and the current planetary embryo. Equations (9) through (16) are used to calculate initial positions and velocities. For reasoning see section 3.2. Radii of the objects are calculated with a defined density ϱ, see also section 3.2 for more details.

Time evolution In the second part the time evolution is calculated by using equation (1-3) to calculate the acceleration of each object and the Strömer-Verlet algorithm (see section 3.1.1). To calculate the first half step needed for the algorithm the Euler method is used. The time interval from zero to the a specified end time is discretized into finite steps of dt. The following procedure is successively repeated for each time step.
First, the algorithm checks whether or not a collision occurred. A collision takes place, if the radii of two objects overlap more than 25%.

No collision The new accelerations are calculated using equation (1-3). The analytically conserved quantities energy, total angular momentum and total momentum are evaluated for each time step. If the current time is within the time interval for which the results are graphically simulated, the current position is saved for later use.

Collision In case of a collision the new initial conditions are calculated. For the object with highest mass the new properties are calculated, all other objects involved in the collision are deleted. Information from previous time steps is retained. The new mass is the sum of the masses of the objects involved in the collision and the new radius is calculated accordingly. The center of mass $\mathbf{R} = \frac{1}{\sum_i m_i} \sum_\mu m_\mu \mathbf{r}_\mu$[2] is evaluated as the new position and the new velocity is chosen to satisfy momentum conservation $\dot{\mathbf{R}} = \frac{1}{\sum_i m_i} \sum_\mu m_\mu \dot{\mathbf{r}}_\mu$[2]. Afterwards the program follows the same procedure as if no collision occurred.

Simulation For the simulation the package vpython is used. Figure 1 shows two snapshots of the planetary embryos orbiting the sun. One at the beginning at $t = 1$ and another one after some time has past at $t = 100$. The red axes represents the xy-plane while the grey axis represents the z-direction. As one can see in Figure 1, after 100 years collisions transpired and the number of planets decreased, while their masses and consequently their radii increased.
Next to the simulation of the time evolution, three graphs, see figure 2, show the analytical conserved quantities total momentum, total angular momentum and total energy. The red dots represent collisions. Total angular momentum and total energy are not conserved after collisions.

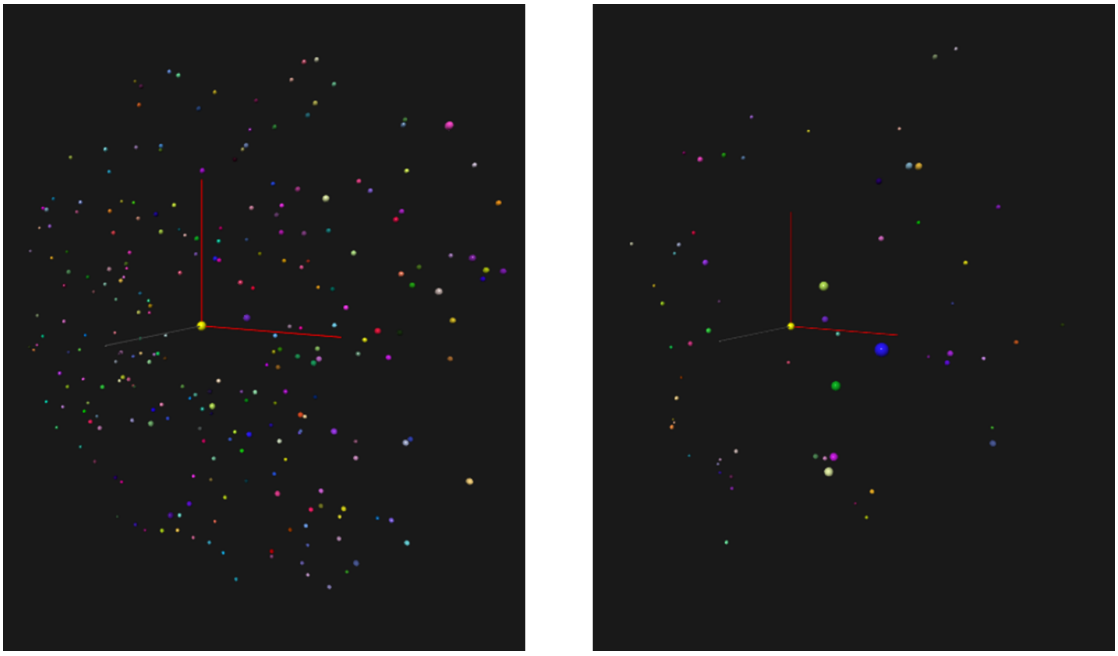

Figure 1: Screenshot of the simulation. Simulation parameters: $m_{min} = 0.5 \cdot 10^{-5} m_{sun}$, $m_{max} = 1.5 \cdot 10^{-5} m_{sun}$, $d_{min} = 0.7AU$, $d_{max} = 4AU$, $m_{star} = 1m_{sun}$, $\epsilon = 0$, $inclination = 3$, $dt = 0.01a$. Left: $t = 1a$, Right: $t = 100a$

3.1.1 Integration algorithm

The Strömer-Verlet-algorithm was chosen since it conserves momentum and angular momentum exactly. It is also symplectic. The Strömer Verlet method is a two step method. In contrast to the second order Runge-Kutta method the global error grows linearly instead of quadratic.[4]
It is possible to find algorithms which conserve energy exactly, however this often results in higher computational costs and it is not possible to conserve sympecticity, energy and momentum simultaneously.[10]

3.2 Initial condition

An estimate for the number of planetary embryos forming during terrestrial growth is given in [8] at 30-50 for massive objects or 500-1000 if the average mass corresponds to one lunar mass. Planetesimals were neglected in this thesis due to computational time. For simplicity a uniform distribution of mass was assumed, not considering a surface density profile as in [8]. Minimal and maximal planet embryos masses where chosen in accordance with the fact, that at this stage the primordial Solar System contained $5m_{earth}$ of solid material between the orbits of Mercury and Jupiter.[5] Another constraint is the lunar mass as a minimal mass.[5]
Maximal eccentricities of 0.02 and maximal inclination of 1° as well as distances to the sun between 0.5AU and 5Au have been chosen according to [8]
The density ϱ is chosen in such a way, the planetary embryos are visible during the simulation and also to allow for the formation of planets within a much smaller timescale

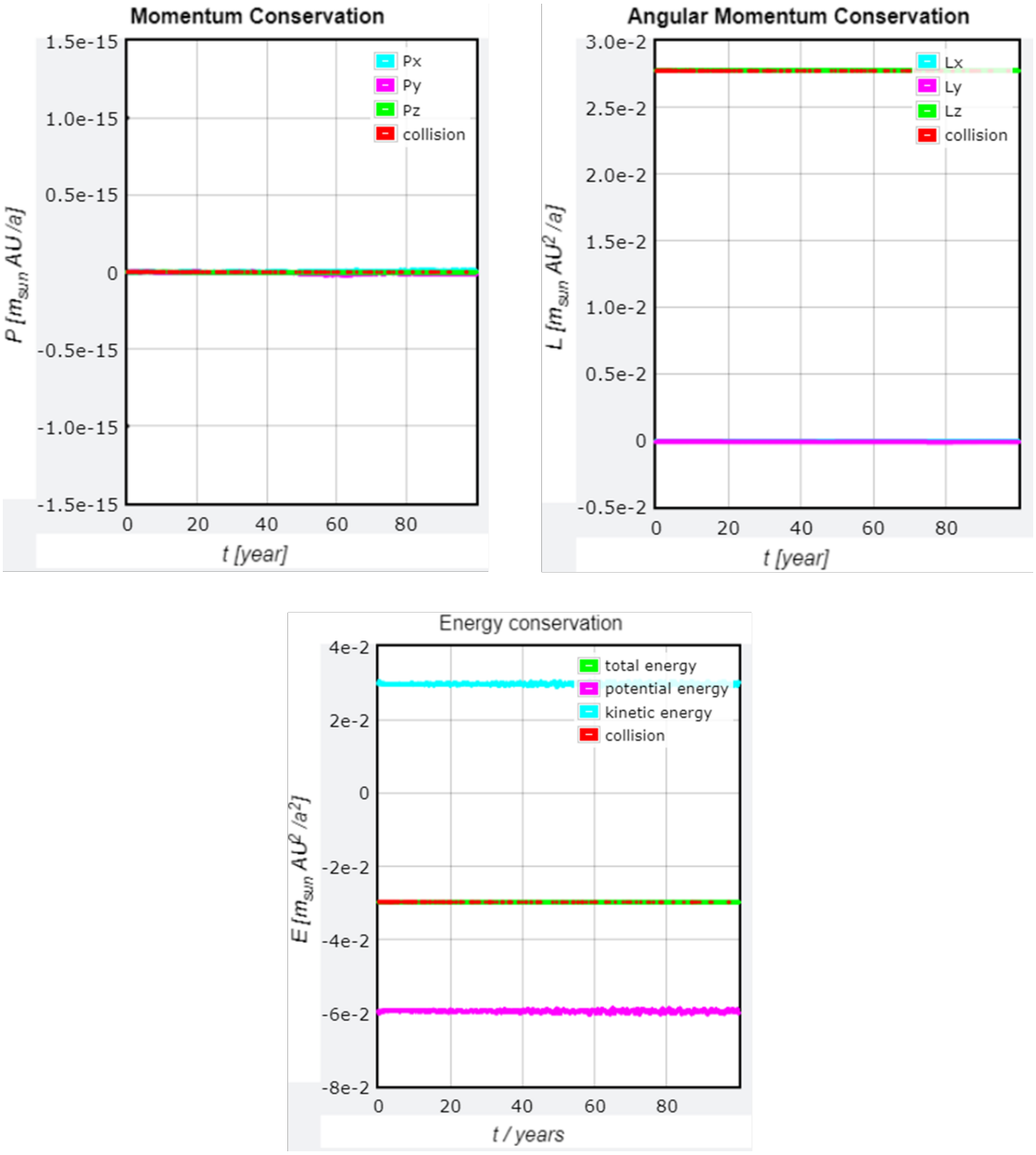

Figure 2: Screenshot of the graphs representing the conserved quantities in the simulation. Simulation parameters: $m_{min} = 0.5 \cdot 10^{-5} m_{sun}$, $m_{max} = 1.5 \cdot 10^{-5} m_{sun}$, $d_{min} = 0.7AU$, $d_{max} = 4AU$, $m_{star} = 1m_{sun}$, $\epsilon = 0$, $inclination = 3$, $dt = 0.01$a. Top left: Total momentum, Top right: Total angular momentum, Bottom: Total energy

than a more realistic one of the order or 10^8 years mentioned in [6].

3.3 Accuracy

The accuracy of the results are examined by comparing to the analytical solution of the two body problem and studying whether or not the integrals are conserved.

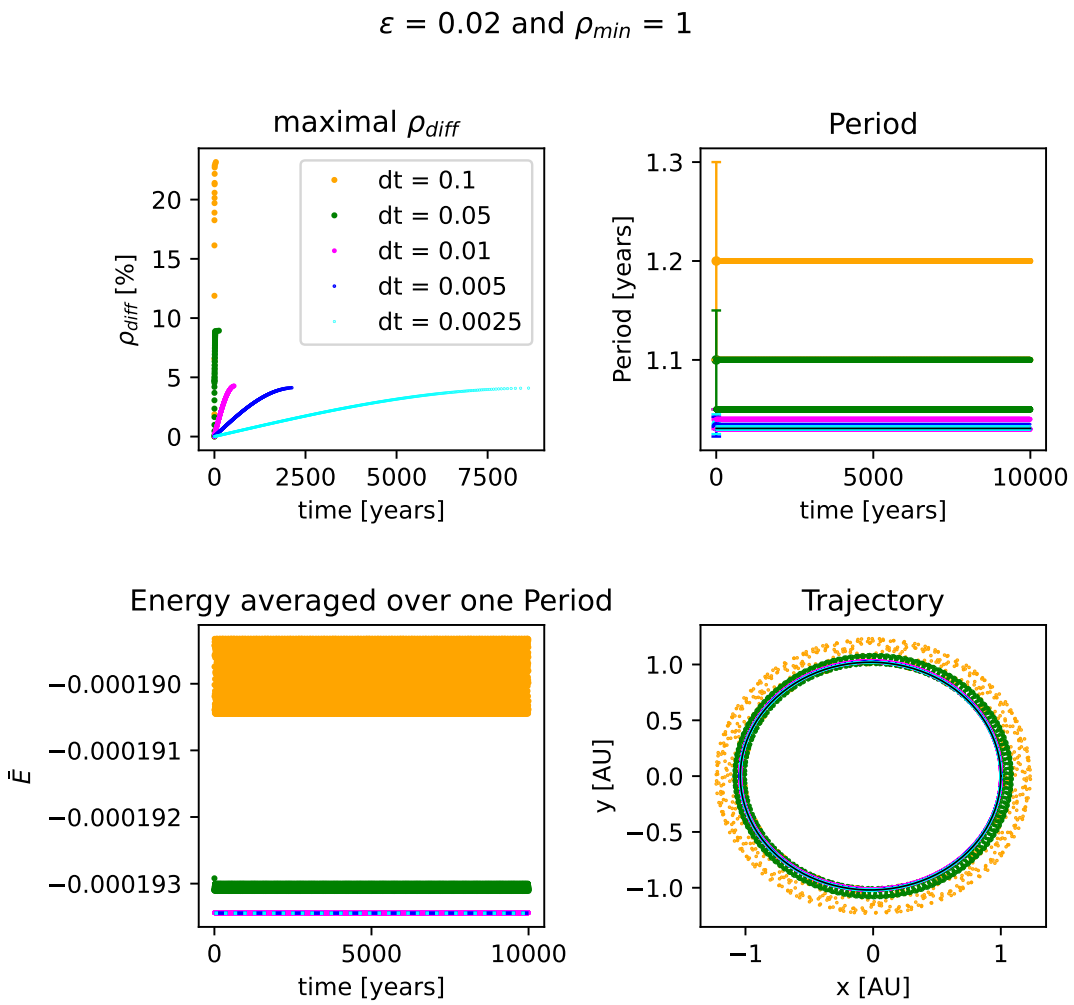

Figure 3: The figure shows the evolution of different quantities over time with different time steps dt. Maximal ρ_{diff} shows the maximal difference of ρ compared to the analytic solution over time. Period describes sidereal period of $\mathbf{r}$, error bars are given by the size of one time step. Energy averaged over one Period shows the average of E in units of $\frac{m_{sun}AU^2}{a^2}$. Trajectory shows the trajectory of $\mathbf{r}$ over 100 Periods. The black line in Period and Trajectory give the analytic solution.

3.3.1 Two Body Problem

To test the accuracy of the program, the results are compared to the analytical solution of the two body problem. In the following the results are shown for different time steps dt, as well as the effect of different initial conditions.
In this section the masses are given by $m_1 = 1m_{sun}$ and $m_2 = 10^{-5}m_{sun}$ representing a planet revolving around the sun. The integration is carried out for up to 10^4 years. The initial conditions for $\phi = 0$ are calculated given a specific $\rho(0) = \rho_{min}$ and ϵ. Equations (9) through (16) are used to calculate initial positions and velocities of the two bodies.

Table 1: maximal error in rho after 10^4 years with $\rho_{min} = 1$ and $\epsilon = 0.02$
dt: size of time step, ρ_{diff}: error of ρ

dt [years]	ρ_{diff} [%]
0.1	23.17
0.05	8.94
0.01	4.27
0.005	4.12
0.0025	4.09

In figure 3 different quantities are shown to evaluate the accuracy of the algorithm for various time steps. ρ and ϵ where chosen according to typical orbits in the solar system , see section 3.2. To estimate the divergent from the analytic solution the difference between the numeric and analytic values of $\rho(\phi)$ are compared: $\rho_{diff} = \frac{|\rho_{analytic}(\phi) - \rho_{numeric}(\phi)|}{\rho_{analytic}(\phi)}$.

As can be seen from the first graph in figure 3 the error of $\rho(\phi)$ reaches its maximum after some finite time smaller than 10^4 years. The larger dt the faster the maximum error is reached and the larger its value.
The period seems to be stable when using the Strömer-Verlet method for the two body problem, with some error due to the finite size of the time step. However, it only comes close to the analytical value for $dt \leq 0.01$
The Strömer-Verlet algorithm in general does not conserve energy, see section 3.1.1. Especially for $dt > 0.01$ large oscillation can be seen even for the averaged energy. Smaller values of dt seem to resemble the integral of energy more closely.
Due to the arguments above in general dt will be chosen ≤ 0.01.
The runtime is of $O(\frac{1}{dt})$, see section 3.4. For a time $> 10^3$ years errors for $dt = 0.01, 0.005, 0.0025$ are of the same order of magnitude, as can be seen in figure 3. Table 3.3.1 shows that for $dt < 0.01$ there is no significant decrease of the maximum error. Therefore, to minimize computational cost unless stated otherwise $dt = 0.01$ is used.

In figure 4 one can see two different effects contributing to the error. Parameters have been chosen for illustrative purposes, the behaviour is analogous for $\rho > 0.3$, $\epsilon < 0.9$ and $dt = 0.01$.
First, the shapes of the ellipses don't overlap. As one can see from equation (16) the eccentricity depends on the energy. The numerically calculated energy however, oscillates with the orbital period $\tau_{numeric} = 3.09a$. Since at $\frac{\tau_{numeric}}{2}$ the energy is higher than $E_{analytic} = E_{numeric}(0)$ the turning point ρ_{max} is larger than for the analytic solution. The fact that energy is not conserved with the Strömer-Verlet algorithm (see section 3.1.1) is therefore, responsible for the deformation of the ellipses.
Furthermore, the numeric trajectory has apsidal precession. The analytic solution of the mere two body problem does not have precession. The apsidal precession arises due to small perturbations[2] in this case caused by the finite time step size. While for the two body problem it is clear, that especially for large ϵ this will lead to substantial deviation from the analytic solution its effect on the n-body problem isn't. Since, for n-planetary bodies revolving around the sun the interacting force between the planets can be seen as a perturbation of the potential of the two body problem.[2] It is difficult to say, whether or not the apsidal precession due to the finite step size is small compared to the apsidal

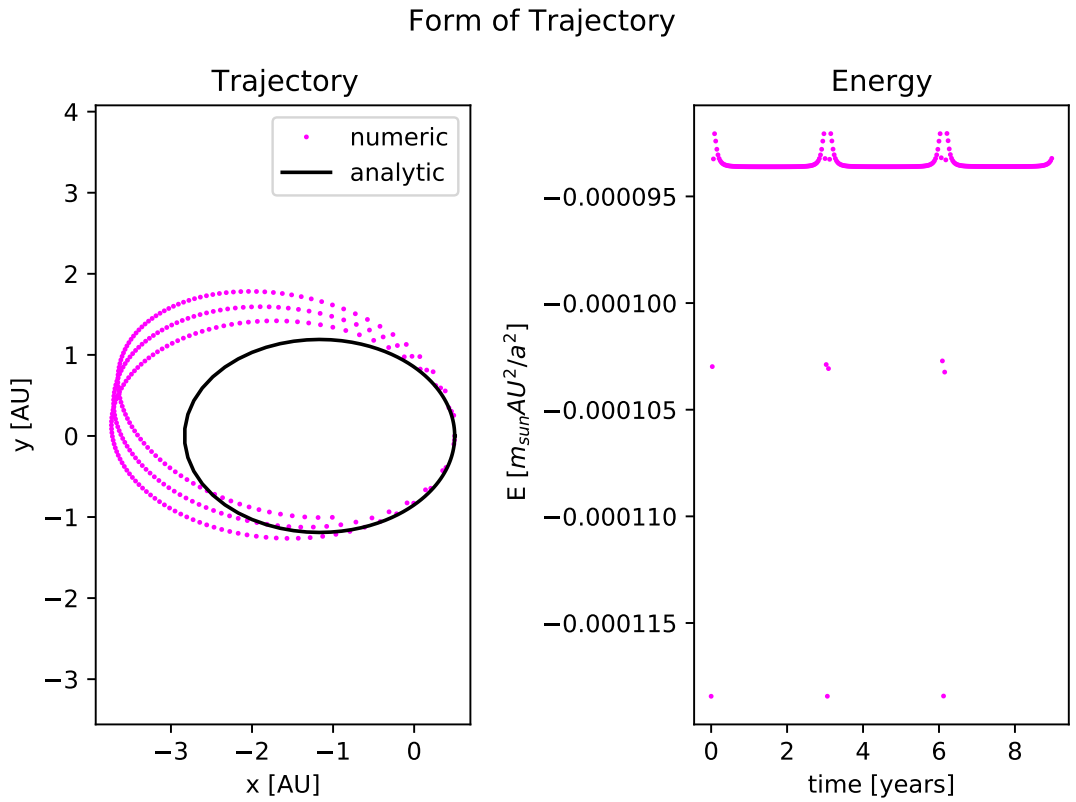

Figure 4: Trajectory and energy for $\rho_{min} = 0.5AU$, $\epsilon = 0.7$, $dt = 0.03a$

precession because of additional planets in the system.

As can be seen from Figure 5 the accuracy of the calculations strongly depends on the initial conditions. A smaller distance leads to larger errors. One reason for this is, that the planets mass is constant. Therefore, the one with the smaller ellipse will be faster and a larger distance is covered during each time step dt. Since, the acceleration depends on the position, this will make the numerical integration less accurate.
The dependency on ϵ is not as easily explained. The higher the eccentricity the larger the oscillations of energy. For the three different eccentricities these change by at least one order of magnitude. A change in energy will also lead to a deformation of the ellipse as can be seen in 4. Eccentricities and energy are connected through equation (16)
For $\epsilon = 0.00, 0.02$ the errors are of the order of 10^{-2} for the trajectories and relative energy oscillations are not larger than 10^{-3}. For the initial conditions relevant for this system (see section 3.2) the results are therefore, viable. Per contra, larger eccentricities have to be treated with care and minimal distances have to be considered to estimate the solutions viability. Since, adding planets to a one planet sun system can be treated as a perturbation [2], a change in order of magnitudes of ϵ is deemed to be unlikely. However, this assumption may need further investigation.

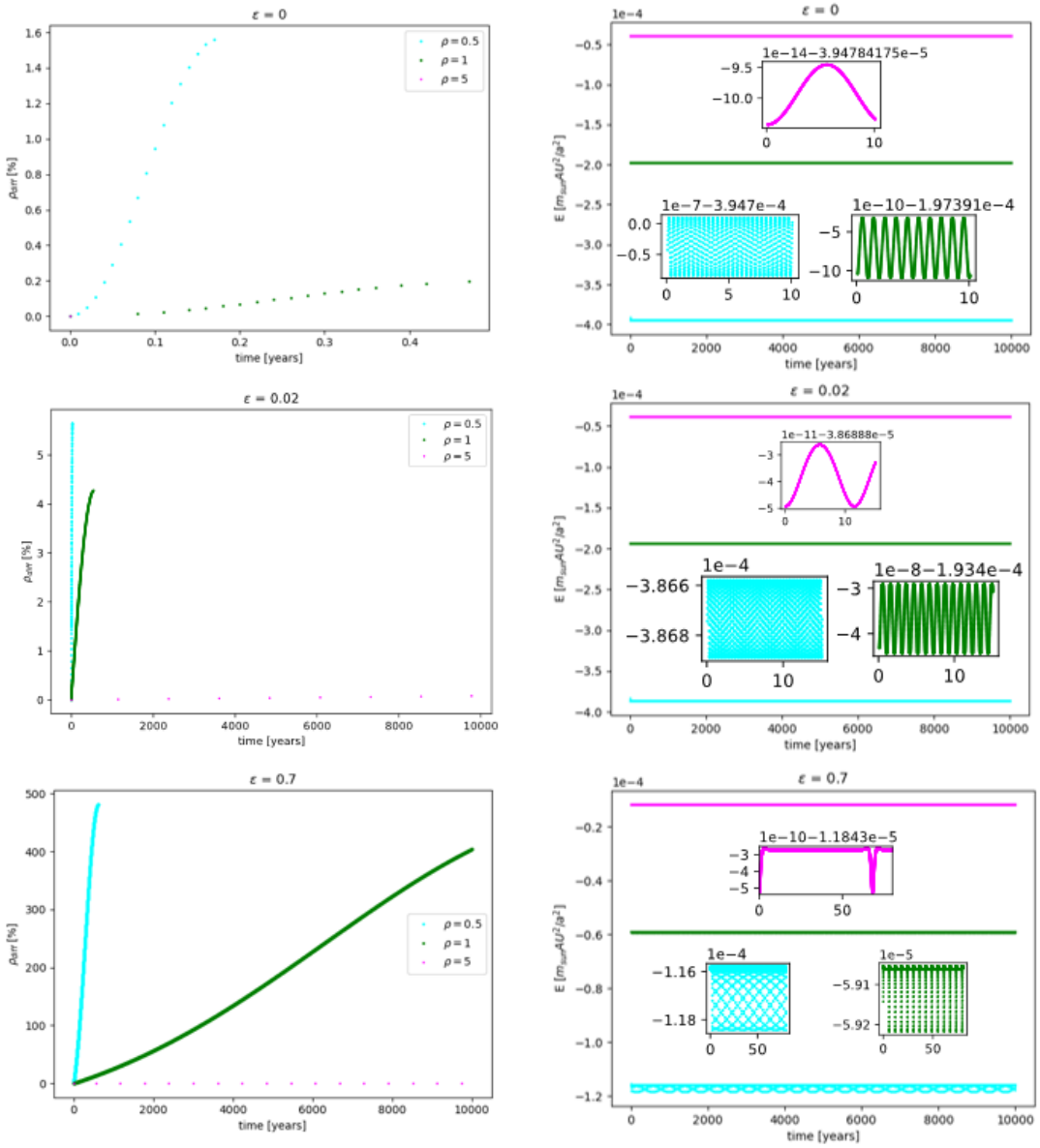

Figure 5: This figure shows the maximal ρ_{diff} and energy for $\epsilon = 0.00, 0.02, 0.7$ and $\rho_{min} = 0.5, 1, 5$ AU.The system was integrated over 10000 years. On the left side maximal ρ_{diff} is shown on the right side the total energy can be seen. The inlays are magnified snippets to show the energy oscillations.

3.3.2 Integrals

Analytically total momentum, total angular momentum and energy should be conserved, see equation (5-7). To estimate the accuracy of the program over time a system with 50 planets and no collisions was evaluated over 100 000 years. The corresponding integrals are shown in figure 6.

As discussed in section 3.1.1 the Strömer-Verlet method conserves total momentum and total angular momentum. The maximal fluctuations from $\mathbf{0}$ in $\mathbf{P}$ are of order 10^{-17}

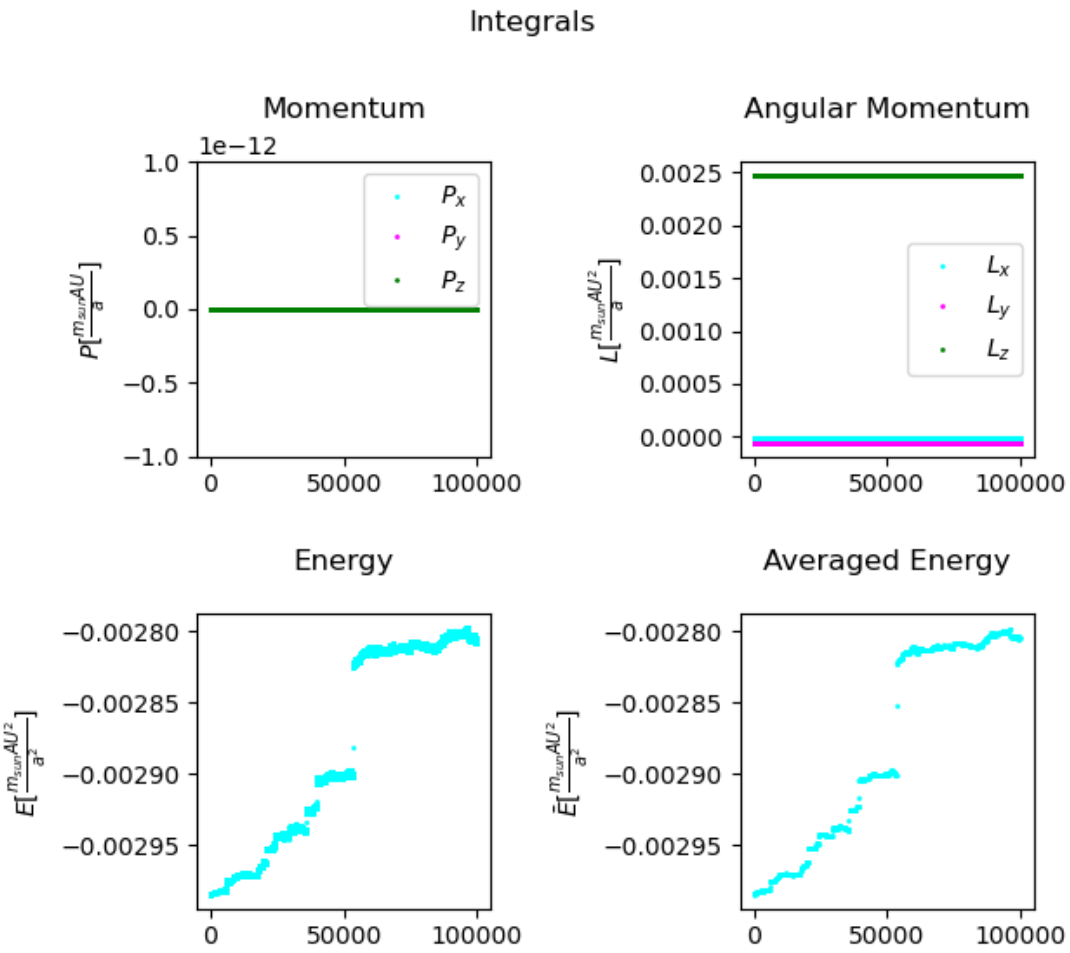

Figure 6: Integrals over a time of 100 000 years, for 50 planets and no collisions. Average energy is the energy averaged over 100 years.

and the maximal relative fluctuation in **L** are of the order of 10^{-9}. This is also reflected with the upper two graphs in figure 6.
In the two lower graphs in figure 6 one can see that energy as well as the averaged energy both drift to higher values and the solution becomes unstable. However, the relative change at $t = 10^5 a$ is 6.3% and for $t = 5 \cdot 10^4 a$ is 2.8%. Below $t = 2 \cdot 10^4 a$ the relative error is below 1%. So while the energy is not stable, results up to $t = 5 \cdot 10^4 a$ preserve energy well.

The reason for the jumps in energy are not clear. Since, no collision occured the change in energy must be due to numerical errors. One reason for this large jumps instead of a continuous might be the dependence of E on ϵ which is illustrated in figure 5. If due to interactions with other planets or numerical error the eccentricity of an orbit was increased significantly this may cause the energy to jump due to higher numerical errors. If this is the case, allowing collisions may make the solution more stable, since according to [8] collisions will circularize the orbit. However, this was not further investigated.

Table 2: parameters and standard deviation
p_i...parameters of polynomial $\sum_{i=0} p_i x^i$, Δp_i...standard deviation of p_i

	p_2 [s]	Δp_2 [s]	p_1 [s]	Δp_1 [s]	p_0 [s]	Δp_0 [s]
with collision t=10 000	0	-	$8.3 \cdot 10^{-2}$	$0.3 \cdot 10^{-2}$	166	4
with collision t=1000	$1.4 \cdot 10^{-5}$	$0.1 \cdot 10^{-5}$	$3.3 \cdot 10^{-2}$	$0.3 \cdot 10^{-2}$	20	2
without collision t=1000	$1.86 \cdot 10^{-2}$	$0.07 \cdot 10^{-2}$	-1.5	0.3	51	21

3.4 Runtime

There are two major parameters which affect the runtime. The number of time steps and the number of planets.
Due to the program structure the program goes linearly with the number of time steps. The parameters determining the number of time steps are the step size and the total time $\#steps = \frac{t}{\Delta t}$.

The dependence on the number of planets n is not as straightforward. Without any collisions between the planets the runtime is of $O(n^2)$ as can be seen from the second graph in figure 7. This is due to the fact, that for calculating the gravitational force the evaluation of a double sum over all planets is necessary.

However, allowing collisions drastically reduces the runtime. This allows the evaluation for n $O(10^3)$ and long time intervals $O(10^4)$ years on a standard desktop computer in a few minutes.
This change in behaviour of the runtime is due to the decreasing number of planets over time. How large the effect is depends on the collision probability, which is indirectly proportional to the density of a planet ϱ and the width of the orbital radius distribution. Furthermore, as can be seen from the first graph in figure 7 the behaviour changes from quadratic to linear, when increasing the time by an order of magnitude. The indicated change is a result of the change in collision frequency over time. Most planets collide early and the number of planets reduces notably within the first few years. For longer time intervals the relative time with many planets is therefore shorter.

The data points where fitted with different polynomials using the python polyfit function for different degrees (up to $O(n^4)$). The best results are given in Table 3.4.
In general it can be said, that the runtime is quadratic. However, allowing collisions will reduce the runtime.

3.5 Effects due to simplifications

In this section the possible effects of assumptions made during this thesis are discussed.

The lower densities of planets leads to a higher collision rate resulting in a faster formation time, than realistic scenarios where the timescale is of order 10^8[6].

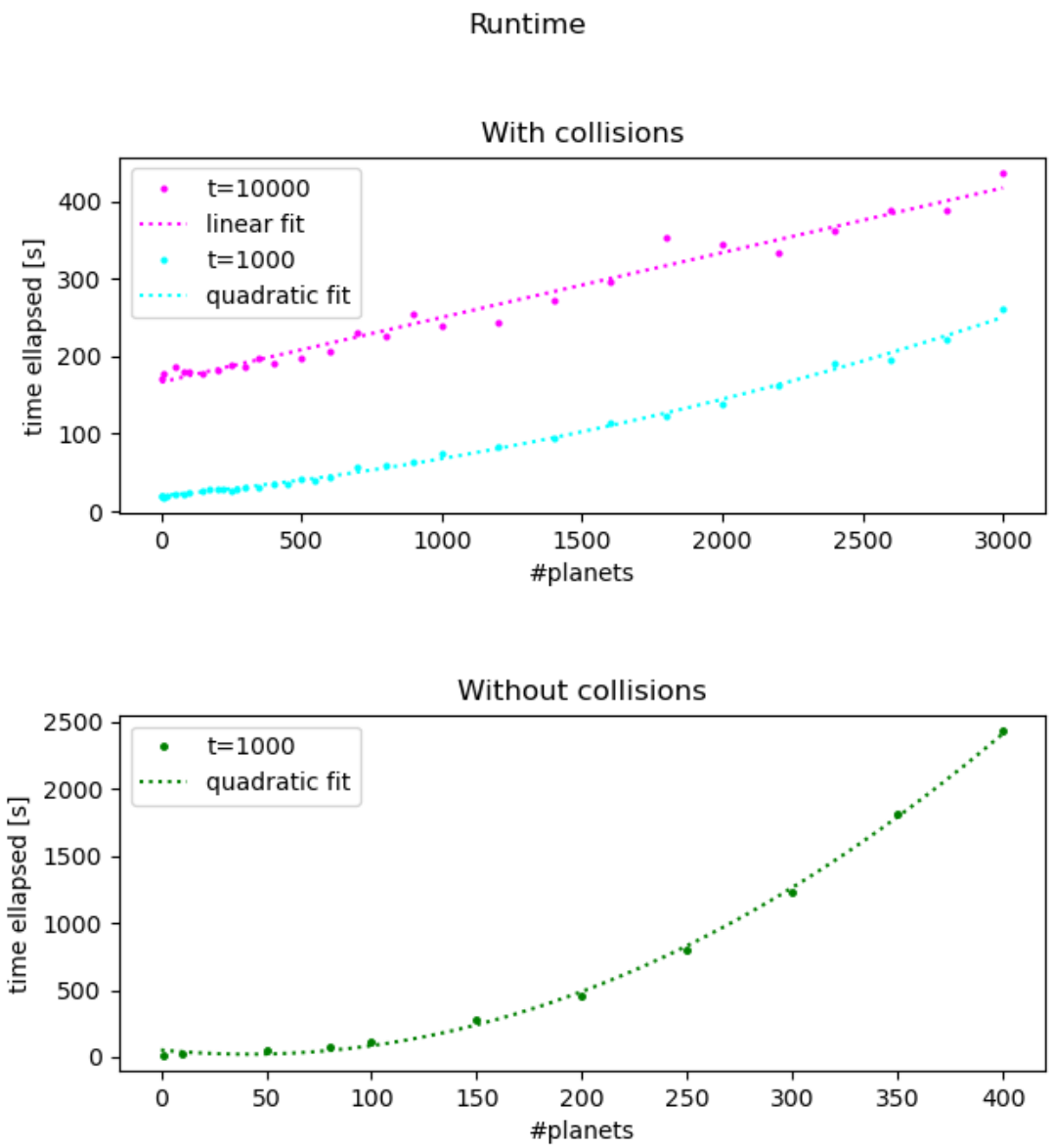

Figure 7: Runtime with and without collision. Except for the density ϱ parameters where chosen according to section 3.2. For the upper graph $\varrho = 3 \cdot 10^{-3} \frac{m_{sun}}{AU^3}$, for the lower one $\varrho = 10^{30} \frac{m_{sun}}{AU^3}$ making collisions almost impossible. Minimal distance to the sun is between 0.5AU and 5AU

The initial mass distribution can strongly affect the final formation process.[8][7] Using a density profile may therefore change the simulation outcome. Observations of protoplanetary discs show different possibilities for the surface density profile.[6]

Including a Jupiter like planet during terrestrial planet formation corresponds closer to the situation during terrestrial planet formation in our solar system.[8] Including a gas giant during terrestrial planets formation plays critical role in shaping the terrestrial

planets.[5]

Interactions with small objects like planetesimals are necessary for the low eccentricity values seen in our solar system.[8] Damping due to drag from a dissipating disk may also play a role in reducing eccentricities.[6]

Treating collsision more accuratly will also effect the outcome of the calculations.[1] If hit and run collisions as well as fragmentation are included the resulting planets masses are lower and eccentricities are smaller.

4 Conclusions

A program for the visualization of a simplified terrestrial planet formation process due to gravitational force and collisions was written. Collisions were handled as totally inelastic. Strömer-Verlet was used as an integration algorithm.

Two pictures of the visualization can be seen in figure 1. As time progresses collisions occur, which reduces the number of planets and increases their size.
The agreement of the simulation with the analytic solution of the two body problem strongly depend on the chosen parameters. It improves with the distance to the star and declines for high eccentricities.
Total momentum and total angular momentum are conserved, while for long integration periods in the order of 10^4 years an upward drift in energy occurs.
In general the runtime for the N-body problem scales quadratically with the number of objects, however allowing collisions affect this behaviour and reduces the runtime.

Possibilities for more realistic simulations include: considering the effects of surface density profile on the initial mass distribution, inserting a Jupiter like planet at the start of the simulation, involving planetesimals and describing collisions more accurately.

5 Bibliography

[1] JE Chambers. "Late-stage planetary accretion including hit-and-run collisions and fragmentation". In: *Icarus* 224.1 (2013), pp. 43–56.

[2] Torsten Fließbach. *Lehrbuch zur theoretischen Physik*. Springer, 2003.

[3] Herbert Goldstein, Charles Poole, and John Safko. *Classical Mechanics*. Addison Wesley, 2000.

[4] Ernst Hairer, Christian Lubich, and Gerhard Wanner. "Geometric numerical integration illustrated by the Störmer–Verlet method". In: *Acta numerica* 12 (2003), pp. 399–450.

[5] André Izidoro and Sean N. Raymond. "Formation of Terrestrial Planets". In: *Handbook of Exoplanets* (2018), pp. 2365–2423. DOI: 10.1007/978-3-319-55333-7_142. URL: http://dx.doi.org/10.1007/978-3-319-55333-7_142.

[6] Eiichiro Kokubo, Junko Kominami, and Shigeru Ida. "Formation of Terrestrial Planets from Protoplanets. I. Statistics of Basic Dynamical Properties". In: *The Astrophysical Journal* 642.2 (May 2006), pp. 1131–1139. DOI: 10.1086/501448. URL: https://doi.org/10.1086/501448.

[7] S. N. Raymond et al. "Terrestrial Planet Formation at Home and Abroad". In: *Protostars and Planets VI* (2014). DOI: 10.2458/azu_uapress_9780816531240-ch026. URL: http://dx.doi.org/10.2458/azu_uapress_9780816531240-ch026.

[8] Sean N. Raymond, Thomas Quinn, and Jonathan I. Lunine. "High-resolution simulations of the final assembly of Earth-like planets I. Terrestrial accretion and dynamics". In: *Icarus* 183.2 (2006), pp. 265–282. ISSN: 0019-1035. DOI: https://doi.org/10.1016/j.icarus.2006.03.011. URL: https://www.sciencedirect.com/science/article/pii/S0019103506001047.

[9] John R. Taylor. *Classical Mechanics*. University Science Books, 2005.

[10] Jeffrey M Wendlandt and Jerrold E Marsden. "Mechanical integrators derived from a discrete variational principle". In: *Physica D: Nonlinear Phenomena* 106.3-4 (1997), pp. 223–246.